JOURNAL OF GEOPHYSICAL RESEARCH, VOL. 106, NO. B7, PAGES 13,781–13,792, JULY 10, 2001

Mechanical analyses of the emplacement of laccoliths and lopoliths

Hatem Zenzri
Departement de Genie Civil, Ecole Nationale d'Ingenieurs de Tunis, Tunis, Tunisia

Leon M. Keer
Department of Civil Engineering, Northwestern University, Evanston, Illinois

Abstract. Elastic deformations of host rocks during the emplacement within the Earth's crust of magmatic intrusions, such as laccoliths and lopoliths, are analyzed. The present analysis is built upon semianalytic elastic solutions for a pressurized horizontal crack buried between an overburden and a semi-infinite base. The current work improves upon recent analyses by including several important features inherent to the development of laccoliths and lopoliths. First, both elongated intrusions (plane strain case) and circular intrusions (axisymmetric case) are described by the current models. Second, the effect of the difference in elastic moduli between the overburden and the substrate is considered. This difference in elastic moduli is characterized by one of the Dundurs parameters. Third, the stress intensity factor at the tip of the crack is assumed to be zero. Thus the stresses are finite, and the obtained laccolithic shapes are doubly hinged with horizontal slopes at the peripheries, as observed in the field. Fourth, unlike plate bending models, which are commonly used for major laccoliths, the current models describe a full range of ratios of intrusion width to overburden thickness. Numerical results are obtained for different combinations of the geometrical parameters, the material contrast and the driving pressure distributions. Graphs of these results confirm the plate bending model for large laccoliths, support Gilbert's concept pertaining to small laccoliths, permit the prediction of the sill-laccolith transition, allow the analysis of the asymmetry in the vertical displacements above and below the intrusion, and lead to a possible mechanism of deep lopoliths emplacements. Some of the obtained results are compared to the available field data from the Henry Mountains.

1. Introduction

In his report on the geology of the Henry Mountains, *Gilbert* [1887] originated the concept of a laccolith on the basis of his observations while studying many intrusions exposed on the flanks of the Henry Mountains in southeastern Utah, in the central part of the Colorado Plateau. Gilbert suggested that a mechanical barrier, a few kilometers beneath the Earth's surface, stops the magmatic intrusion in the Henry Mountains. Thus the magma, after propagating vertically through planar dikes, insinuates itself laterally between two strata, forming a horizontal thin sill which can inflate and expand into a laccolith having a flat floor and arched roof. Laccoliths gain their large thickness by causing the overburden to lift and bend. According to *Corry* [1988], lopoliths form at greater depths than laccoliths and result from sills that inflate by depressing the floor. Whereas lopolith models are rare, many mechanical models, supported by direct observations of the Earth surface deformation, were devoted to laccolith emplacements by roof lifting [e.g., *Pollard and Johnson*, 1973; *Turcotte and Schubert*, 1982; *Corry*, 1988; *Jackson and Pollard*, 1988, 1990; *Guterman et al.*, 1996; *Kerr and Pollard*, 1998]. The geophysical purpose of such models is to provide an understanding of the laccolith's formation stages. Analysis of the stability of the dome-shaped structure over magmatic chambers, which is related to the stresses around the intrusion, is also of a major geophysical interest since under certain conditions the growth of the dome can develop into a seismic event [*Guterman et al.*, 1996]. The current work focuses on the mechanical modeling of elastic deformation in the media surrounding a magmatic intrusion.

In published laccolith analyses, two main types of mechanical models have been used: crack models and plate bending models. When using the linear elastic plate bending theory of *Timoshenko and Woinowsky-Kriegler* [1959], the ratio of intrusion width (diameter) to overburden thickness should be very large ($\gtrsim$10). For laccoliths this ratio is rarely that large. Indeed, in the Henry Mountains the overburden is 3 to 4 km thick, while one of the largest domes, situated in the eastern flank of Mount Hillers, has a roughly circular plane shape with a diameter of ~14 km [*Jackson and Pollard*, 1988]. However, *Pollard and Johnson* [1973] considered that during the intrusion emplacement the stack of layers forming the overburden behaves mechanically as a single layer having the same bending rigidity as the multilayer. When the Young's modulus of the single layer is fixed to the greatest modulus in the stack, the thickness of the single layer, which is called the effective thickness, is smaller than the total thickness of the stack of layers. The effective thickness is minimum when the layers are free sliding and maximum when they are perfectly bonded. The effective thickness over the Buckorn Ridge intrusion, which has a diameter of ~10 km and is on the eastern flank of Mount

Paper number 2001JB000319.
0148-0227/01/2001JB000319$09.00

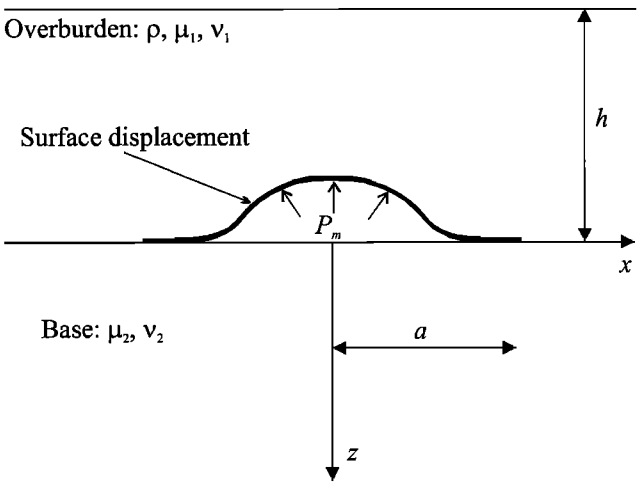

Figure 1. Idealization of the magmatic intrusion emplacement (case of a laccolith).

Holmes in the Henry Mountains, is estimated to be between 1400 and 300 m [*Pollard and Johnson*, 1973, p. 323]. Nevertheless, for small laccoliths with diameters of ~1 km, such as the Trachyte Mesa intrusion and the Black Mesa intrusion on the eastern flank of Mount Hillers [*Johnson and Pollard*, 1973, Figure 4], the ratios of diameters to effective thicknesses are smaller than the 10 required for beam or plate theory. In addition, when using the plate model, only upward displacements can be computed, and that constitutes a second limitation of this model since it is inapplicable to lopoliths or hybrid intrusions.

In published laccolith analyses using the crack model the ratio of intrusion width to overburden thickness can cover a large range of values. *Pollard and Holzhausen* [1979] developed a plane strain crack model to study the mechanical interaction between a fluid-filled fracture and the Earth's surface. In Pollard and Holzhausen's paper the overburden and the base are of identical materials, the width of the fracture is prescribed, and the stresses around the intrusion are singular. *Guterman et al.* [1996] presented solutions for stresses and displacements due to a uniformly pressurized circular crack in a homogeneous half-space with applications to deformations associated with sill intrusions. The stresses around the intrusion in Guterman et al.'s paper are also singular, and the equilibrium state is viewed as corresponding to the crack at the threshold of being destabilized. Thus the stress intensity factor is equated to the tensile strength of the encompassing rocks, and therefore a relationship between the excess pressure and the crack's diameter is imposed. Such singular solutions combined with hydrodynamic aspects of magma flow are relevant to the analyses of the mechanical relationship between pressurization and the fracture process, which is not the aim of this paper.

The present analysis builds upon a crack model to simulate the initial doming and sinking of the rocks encompassing laccoliths and lopoliths. The intrusion is viewed as a horizontal crack subjected to a magmatic pressure distribution and buried between a horizontally unbounded overburden and a semi-infinite base (Figure 1). Field and theoretical considerations show that vertical growth of laccoliths occurs by elastic, elastic-plastic, or ductile bending of the roof rocks [*Johnson and Pollard*, 1973; *Pollard and Johnson*, 1973]. The elastic stage largely controls several of the laccolithic shapes and modes of failure observed in the Henry Mountains [*Pollard and Johnson*, 1973]. The theoretical problem is here reconsidered from the point of view of elasticity theory where the plane and the axisymmetric cases are included. These cases represent two limit cases of the elliptical plane shape of the intrusions [*Pollard and Johnson*, 1973, Figure 1]. The contrast in material properties above and below the crack is also taken into consideration. Like the free surface, the material contrast should introduce an asymmetry in the arching of the intrusion roof and floor. Indeed, it is obvious that a crack will inflate by doming the roof when the deeper strata are rigid and by depressing the floor when the upper layers are rigid. The slopes of the surfaces below and over the crack are here assumed to become zero over the peripheries. Such an assumption is frequently used in previous published analyses based on the plate model [*Pollard and Johnson*, 1973; *Kerr and Pollard*, 1998] and is consistent with field observations in the Henry Mountains [*Jackson and Pollard*, 1988, Figures 10 and 14]. Within an elastic crack model a horizontal slope at the tip of the crack corresponds to a nil stress intensity factor and thus finite stresses around the tip of the crack.

The formulation used in this paper employs a suitable representation of the elastic fields by Fourier (plane strain case) and Hankel (axisymmetric case) integrals. Both cases yield a Fredholm integral equation of the second kind for an auxiliary function that is directly related to the vertical displacements of the surrounding medium. In the axisymmetric case the mathematical formulation is close to that developed by *Guterman et al.* [1996], but here the stresses are finite and the material contrast is allowed. The semianalytical approach, chosen here for its simplicity and transparency, has been widely used in the engineering literature. Studies such as those of *Sneddon* [1951], *Srivastava and Singh* [1969], and *Erdogan* [1971], deal with singular stress distributions for prescribed and pressurized tensile crack in an elastic half-space. In other studies, such as those involving contact between an elastic layer and a half-space [*Keer and Chantaramungkorn*, 1972; *Keer et al.*, 1972], the stress distributions are finite and the contact surface is not prescribed.

2. Plane Strain Analysis

The plane elastostatic problem formulated here is that of a horizontally unbounded overburden in shear stress free contact with a semi-infinite base and is the elasticity analysis corresponding to the plate bending approach of [*Kerr and Pollard*, 1998, Figure 1]. Here, the condition of shear stress free contact is used for mathematical convenience. The contact will likely be a slipping contact near the laccolith edge and bonded away from it. The actual case will probably be between fully bonded and shear stress free with most of the physics contained in the transfer of normal stress. The plane strain assumption means that the vertically thin magmatic intrusion is modeled as a very elongated rectangular strip. The intrusive width is $2a$, the thickness of the overburden is h, and the coordinate system is placed as shown in Figure 1. The shear moduli and Poisson's ratios of the isotropic overburden and base are denoted by μ_1, ν_1, μ_2, and ν_2, respectively. The upper surface of the overburden is free of traction. The overburden and the base are pressed by the magmatic normal traction $P_m(x)$ distributed over the segment $|x| \leq a$. As the intrusion spreads, the two bodies deform, and separation is assumed to take place over the segment $|x| \leq a$, while contact is maintained outside this

interval. The deformations and stresses produced by the intrusion are due to the driving pressure $P(x) = P_m(x) - \rho gh$, where ρ is the density of the overburden and g is the acceleration of gravity.

The three components of the stress tensor and the horizontal and vertical displacements produced by the intrusion are denoted by σ_{xx}, σ_{xz}, σ_{zz}, μ_x, and u_z, respectively. A solution is sought, therefore, to the problem stated by the following boundary conditions:

On $z = -h$

$$\sigma_{xz}^1 = 0, \qquad 0 \le |x| < \infty, \tag{1}$$

$$\sigma_{zz}^1 = 0, \qquad 0 \le |x| < \infty, \tag{2}$$

On $z = 0$

$$\sigma_{xz}^1 = 0, \qquad 0 \le |x| < \infty, \tag{3}$$

$$\sigma_{xz}^2 = 0, \qquad 0 \le |x| < \infty, \tag{4}$$

$$\sigma_{zz}^1 = \sigma_{zz}^2, \qquad 0 \le |x| < \infty, \tag{5}$$

$$u_z^1 = u_z^2, \qquad a < |x| < \infty, \tag{6}$$

$$\sigma_{zz}^1 = -P(x), \quad 0 \le |x| < a. \tag{7}$$

A further constraint will require that the stresses are bounded at the tips $|x| = a^+$. The superscripts 1 and 2 in (1)–(7) refer to the overburden and base, respectively. Using the Fourier transforms and the symmetries of the problem, the displacement solution is written [*Sneddon*, 1951, chapter 9] as

$$u_x^i = \frac{1}{\pi\mu_i}\int_0^\infty \left[(1-\nu_i)\frac{\partial^2 G^i}{\partial z^2}(z,t) + \nu_i t^2 G^i(z,t)\right]\frac{\sin(tx)}{t}\,dt \tag{8}$$

$$u_z^i = \frac{1}{\pi\mu_i}\int_0^\infty \left[(1-\nu_i)\frac{\partial^3 G^i}{\partial z^3}(z,t) - (2-\nu_i)t^2\frac{\partial G^i}{\partial z}(z,t)\right]\frac{\cos(tx)}{t^2}\,dt, \tag{9}$$

where

$$G^i(z,t) = [A^i(t) + zB^i(t)]e^{-tz} + [C^i(t) + zD^i(t)]e^{tz}. \tag{10}$$

The subscript or superscript i in (8)–(10) is 1 for the overburden and 2 for the base.

The functions $A^i(t)$, $B^i(t)$, $C^i(t)$, $D^i(t)$ in (10) are to be determined from the boundary conditions, and the derived solution must be such that all the stress components tend to zero as z tends to infinity, which last condition leads to $C^2(t) = D^2(t) = 0$. The boundary conditions given by (1)–(5) lead to algebraic relations from which each of the functions $B^1(t)$, $C^1(t)$, $D^1(t)$, $A^2(t)$, $B^2(t)$ is expressed in terms of the function $A^1(t)$, and these expressions are given by (A1)–(A5) in Appendix A.

The remaining two boundary conditions (6) and (7) are mixed. Following *Keer and Chantaramungkorn* [1972] and *Keer et al.* [1972], it can be shown that (6) is automatically satisfied by setting

$$E(t) = \int_0^a sH(s)J_0(ts)\,ds, \tag{11}$$

where J_0 is the Bessel function of the first kind of order zero, $E(t)$ is expressed in terms of $A^1(t)$ in (A7) in Appendix A, and $H(s)$ is directly related to the displacements in the zone of separation as

$$u_z^1 - u_z^2 = \int_x^a \frac{sH(s)}{\sqrt{s^2 - x^2}}\,ds, \qquad z = 0, \qquad 0 < |x| < a. \tag{12}$$

The last boundary condition (equation (7)) leads to the following Fredholm integral equation of the second kind for the auxiliary function $H(s)$:

$$H(s) - \int_0^a K(t,s)H(t)\,dt = F(s), \qquad 0 \le |s| < a, \tag{13}$$

where

$$K(t,s) = (1+\theta)t \cdot \int_0^\infty \frac{[(1+2\lambda h+2\lambda^2h^2)e^{2\lambda h} - 1]\lambda J_0(\lambda s)J_0(\lambda t)d\lambda}{e^{4\pi h} + [\theta(1+2\lambda h+2\lambda^2h^2) - (1-2\lambda h+2\lambda^2h^2)]e^{2\lambda h} - \theta} \tag{14}$$

$$F(s) = -\frac{4(1-\nu_1)}{\pi(1+\theta)\mu_1}\int_0^s \frac{P(\lambda)}{\sqrt{s^2-\lambda^2}}\,d\lambda. \tag{15}$$

The parameter θ in (14) and (15) is defined by

$$\theta = \frac{\mu_2(1-\nu_1) - \mu_1(1-\nu_2)}{\mu_2(1-\nu_1) + \mu_1(1-\nu_2)}, \tag{16}$$

and it is one of Dundurs parameters that usually appear when solving certain two-material problems in elasticity [*Dundurs and Stippes*, 1970; *Keer and Chantaramungkorn*, 1972; *Keer et al.*, 1972]. Thus $\theta = 1$ corresponds to a rigid base and a compliant overburden; $\theta = 0$ corresponds to an overburden and base of identical materials; $\theta = -1$ corresponds to a rigid overburden and a compliant base. Note that for $\theta = -1$ the ratio $(1-\nu_1)/(1+\theta)\mu_1$ appearing in (15) should be replaced by $(1-\nu_2)/(1-\theta)\mu_2$. More mathematical details for the derivation of (13)–(15) are given in Appendix A.

In order that the contact stress is bounded at $|x| = a^+$, the further condition,

$$H(a) = 0 \tag{17}$$

must be applied (see Appendix A). Equation (17) provides a supplementary relation between the intrusive width ($2a$), the vertical displacements, and the driving pressure.

The driving pressure obviously depends on the nature of the magma and its source. According to *Johnson and Pollard* [1973], when considering the intrusions in the Henry Mountains, the physical magma properties are not exactly known, and these properties have changed considerably during intrusion and crystallization. *Johnson and Pollard* [1973] selected three rheological models (Newtonian viscous, pseudoplastic, Bingham) which represent the behavior of magma under different conditions. They concluded that for intruding magma

the driving pressure drops toward the intrusion tip for all three types. Also, while the driving pressure has to be constant for static Newtonian or pseudoplastic, a static Bingham magma may have a residual pressure which varies along the width of the intrusion. It is also true that a Newtonian magma may crystallize with a nonuniform pressure distribution if it freezes as it flows. In many published analyses dealing with the developments of laccoliths [*Pollard and Johnson*, 1973; *Pollard and Holzhausen*, 1979; *Kerr and Pollard*, 1998], both uniform pressure and varying pressure distributions are considered. Configurations obtained at the elastic stage of formation with varying pressure distributions for intruding Newtonian or pseudoplastic magma certainly cannot be preserved when the magma comes to a rest. However and more generally, configurations attained at the bending stage of a laccolith formation are rarely preserved and are generally followed by a faulting stage at the end of which an equilibrium form is reached. The faulting stage begins over the periphery of the intrusion, stops the lateral growth of the magma, and favors the uplift of the overburden. For example, the maximal vertical displacement reached after the bending stage in the Black Mesa intrusion in the Henry Mountains is estimated to be ~50 m, while the thickness at the equilibrium form is ~200 m [*Pollard and Johnson*, 1973, Figure 25]. According to *Pollard and Johnson* [1973, p. 352], when the intrusion reaches the final thickness the driving pressure is compensated by the magma weight and static equilibrium prevails while the magma crystallizes. The Buckorn Ridge intrusion (diameter ≈ 10 km) and the Mount Hillers intrusion (diameter ≈ 14 km), which are major laccoliths present thicknesses of ~1.2 km and ~2.5 km, respectively. These thicknesses are certainly far from the elastic stages.

Following *Kerr and Pollard* [1998], the driving pressure is assumed here to vary as decreasing toward the periphery of the intrusion, i.e.,

$$P(x) = p(1 - |x/a|^n) - q. \tag{18}$$

According to Kerr and Pollard, q is the lithostatic pressure ($q = \rho g h$) and the magmatic pressure is $P_m(x) = p(1 - |x/a|^n)$. This distribution may only mimic the magmatic pressure drop along the intrusion and is mainly used for mathematical convenience. However, when considering Figure 1 and especially the tip of the intrusion with a horizontal slope, it appears that the driving pressure $P(x)$ must vary along the intrusion width. To ensure the uplift of the overburden, while maintaining contact between the base and the overburden at the periphery of the intrusion, it is necessary that the driving pressure $P(x)$ is positive around the center of the intrusion and negative at the periphery. Thus the magmatic pressure $P_m(x)$ has to be larger than the lithostatic pressure in the vicinity of the center of the intrusion and smaller than it at the periphery. The distributions of $P_m(x)$ for different values of n were presented by *Kerr and Pollard* [1998, Figure 2]. The mathematical form of the driving pressure distribution (equation (18)) includes many situations and especially those used in previous laccolith studies. Indeed, for large values of n the magmatic pressure approaches a uniform value, whereas the case $n = 1$ corresponds to the linear distribution frequently considered [*Pollard and Johnson*, 1973; *Pollard and Holzhausen*, 1979]. Small values of n approach the point load case, which was also considered by *Pollard and Johnson* [1973]. The actual pressure distribution lies between the uniform distribution and the point load case and therefore may be approached by one of the distributions represented in (18). Otherwise, zero magmatic pressure at the tip of the intrusion may be related to the fact that the magma does not penetrate the entire domain of a crack during the fracturing process [e.g., *Abé et al.*, 1976]. For equilibrium crack states this nullity may not be necessary. In the following, the idealized driving pressure $P(x)$ proposed by Kerr and Pollard and expressed in (18) is retained with particular attention to the nearly uniform distributions, which are physically significant for any magma, and the linear distribution, which may be significant for Bingham magma.

In order to keep the computations tractable the magmatic pressure at the center of the intrusion, denoted p in (18), is considered unknown and the elastic study is parameterized by the width of the intrusion ($2a$), the overburden thickness (h), the lithostatic pressure (q), the Dundurs parameter θ and the scalar n defining the pressure distribution (equation (18)). The pressure p and the auxiliary function $H(s)$ have to be determined using (13) and (17). (The numerical results are presented in section 4.)

3. Axisymmetric Analysis

The axisymmetric problem considered in this section corresponds to an intrusion with a horizontal circular shape. Figure 1 also serves to show the geometry of the axisymmetric case, and the coordinate x is now a polar coordinate corresponding to radial distance. The boundary conditions written in section 2 (equations (1)–(7)) are still applicable (the absolute value symbol is no longer needed). Using the Hankel transforms, the displacement solution is written [*Sneddon*, 1951, chapter 10]

$$u_x^i = \frac{1}{(1 + 2\nu_i)\mu_i} \int_0^\infty t^2 \frac{\partial G^i}{\partial z}(z, t) J_1(tx)\, dt \tag{19}$$

$$u_z^i = \frac{1}{(1 - 2\nu_i)\mu_i} \int_0^\infty t \left[(1 - 2\nu_i) \frac{\partial^2 G^i}{\partial z^2}(z, t) - 2(1 - \nu_i) t^2 G^i(z, t) \right] J_0(tx)\, dt, \tag{20}$$

where J_0, J_1 are Bessel functions of order zero and one, respectively and, as before,

$$G^i(z, t) = [A^i(t) + zB^i(t)]e^{-tz} + [C^i(t) + zD^i(t)]e^{tz}. \tag{21}$$

In the same manner as that used in the plane strain problem, the boundary conditions lead to $C^2(t) = D^2(t) = 0$ and the expressions of the functions $B^1(t)$, $C^1(t)$, $D^1(t)$, $A^2(t)$, $B^2(t)$, in terms of the function $A^1(t)$ are given in equations (A15)–(A19) in Appendix A. Following *Keer et al.* [1972], it can be shown that (6) is automatically satisfied by setting

$$E(t) = \int_0^a H(s) \sin(ts)\, ds, \tag{22}$$

where $E^1(t)$ is expressed in terms of $A^1(t)$ in (A20) in Appendix A and $H(s)$ is directly related to the displacements in the zone of separation as

$$u_z^1 - u_z^2 = \int_x^a \frac{H(s)}{\sqrt{s^2 - x^2}}\, ds, \qquad z = 0, \qquad 0 < x < a. \tag{23}$$

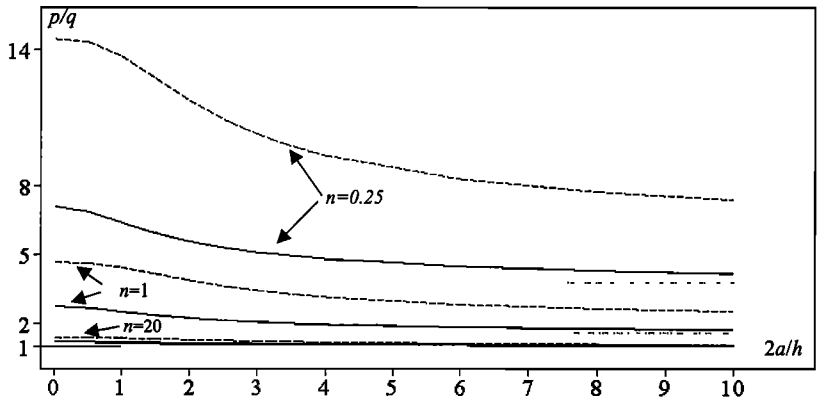

Figure 2. The ratio of the magmatic pressure at the center of the intrusion (p) to the lithostatic pressure (q) versus the geometrical ratio ($2a/h$) for various values of n. (Solid curves, the plane strain case; dashed curves, the axially symmetric case; dotted curves, the *Kerr and Pollard* [1998] result for large geometrical ratios: $p/q = [(n + 1)(n + 3)]/[(n + 1)(n + 3) - 3]$.)

The last boundary condition (7) leads to the following Fredholm integral equation of the second kind for the auxiliary function $H(s)$:

$$H(s) - \int_0^a K(t, s)H(t)\, dt = F(s), \qquad 0 \le s < a, \tag{24}$$

where

$$K(t, s) = \frac{2(1 + \theta)}{\pi} \cdot \int_0^\infty \frac{[(1 + 2\lambda h + 2\lambda^2 h^2)e^{2\lambda h} - 1]\sin(\lambda s)\sin(\lambda t)\, d\lambda}{e^{4\lambda h} + [\theta(1 + 2\lambda h + 2\lambda^2 h^2) - (1 - 2\lambda h + 2\lambda^2 h^2)]e^{2\lambda h} - \theta} \tag{25}$$

$$F(s) = -\frac{4(1 - \nu_1)}{\pi(1 + \theta)\mu_1} \int_0^s \frac{\lambda P(\lambda)}{\sqrt{s^2 - \lambda^2}}\, d\lambda. \tag{26}$$

In order that the contact stress is bounded at $x = a^+$, the condition

$$H(a) = 0 \tag{27}$$

must be satisfied (see Appendix A).

The axially symmetric magmatic pressure distribution is also defined by (18). The pressure p and the auxiliary function $H(s)$ have to be determined using (24) and (27).

4. Numerical Results and Interpretations

Approximating the integrals in (13) by a sum over discrete values of s and using (17), a system of linear equations in the unknowns $H(s_i)$ and p is obtained. After suitable changes, the problem is normalized and solved for the unknowns $[(1 + \theta)\mu_1 H(s_i)]/[q(1 - \nu_1)]$ and p/q, where q is the lithostatic pressure ($q = \rho g h$). The kernel $K(t_i, s_i)$ (equation (14)) of the Fredholm equation is calculated numerically, and all the numerical computations are made using Maple software. The parameters of the problem are then the geometrical ratio $2a/h$, the Dundurs parameter θ, and the scalar n. Since (24) and (27) are of the same form as (13) and (17), the axisymmetric problem is treated in the same way.

4.1. Magmatic Pressure

From (13)–(17) and (24)–(27) it can be easily seen that among the elastic coefficients only the Dundurs parameter may affect the licit pressure p. Otherwise, Young's modulus contrasts (E_2/E_1) for most sedimentary rocks are no smaller than 1/100 and no bigger than 100 [*Pollard and Johnson*, 1973, p. 321]. The ratio 100 corresponds, for example, to sandstones such as the Navajo over interbedded sandstones and shales such as the Morisson formation which are present in the Henry Mountains basin [*Jackson and Pollard*, 1988, Figure 5]. Poisson's ratios are small, <0.5, and when squared their contrast becomes less significant. Then geological significant values of θ ($= \{1 - (E_1/E_2)[(1 - \nu_2^2)/(1 - \nu_1^2)]\} \cdot \{1 + (E_1/E_2)[(1 - \nu_2^2)/(1 - \nu_1^2)]\}^{-1}$) lie between (−0.99) and (0.99). If the contrast (E_2/E_1) is considered between 1/2 and 2, θ lies between (−1/3) and (1/3). The numerical results obtained with the current models for both plane strain and axisymmetric cases showed that when θ is between (−0.99) and (0.99), there is no significant dependence of the licit pressure p on the Dundurs parameter θ. Thus the elastic properties of the materials have essentially no constraint on the magmatic pressure needed to inflate an intrusion of a given width.

The values of p/q calculated for various geometrical ratios $2a/h$ and three distributions of the driving pressure (n = 20, 1, 1/4) are given in Figure 2. To make the figures readable, the results are presented in the form of curves of constant n. Such curves should not be associated with the intrusion's growth since the present study is not addressing time-dependent growth. For large laccoliths a comparison with the previously published results using the thin plate model can be made. In the plane strain case the ratios

$$p/q = \frac{(n + 1)(n + 3)}{(n + 1)(n + 3) - 3} \tag{28}$$

obtained by *Kerr and Pollard* [1998, equation (14)] with the beam plate model appear here as limiting values for the con-

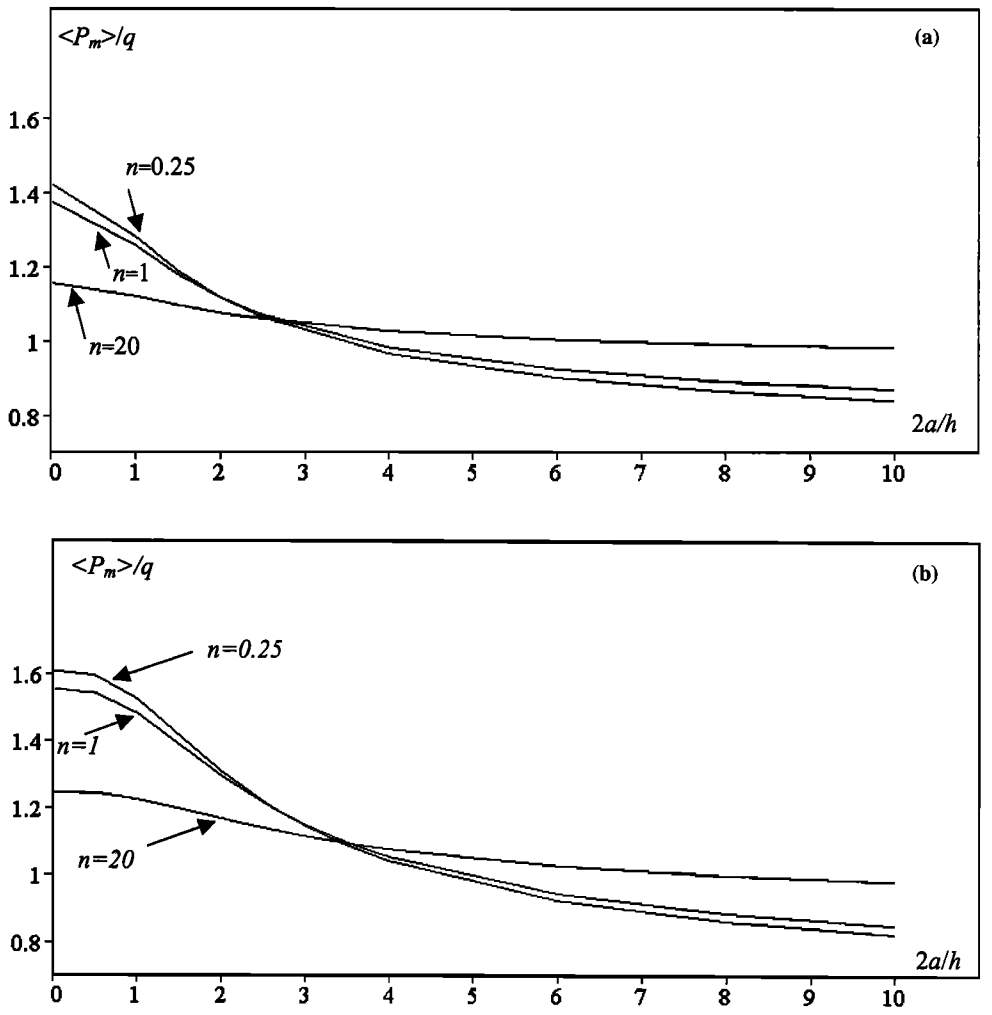

Figure 3. The ratio of the magmatic pressure averaged over the intrusion area ($\langle P_m \rangle$) to the lithostatic pressure (q) versus the geometrical ratio ($2a/h$) for various values of n. (a) The plane strain case. (b) The axially symmetric case.

stant n curves shown in Figure 2. Kerr and Pollard obtained (28) by solving the plane strain problem of a plate subjected to the driving pressure distribution $P(x)$ along the intrusion's width with nil displacement, rotation, and bending moment at the tips of the intrusion. From (28), which is valid for large geometrical ratios, one can note that for a uniform magmatic pressure distribution ($n \to \infty$) the only solution is $p = q$ and the opening of the intrusion is zero. Equation (28) and Figure 2 show that the magmatic pressure at the center of the intrusion is greater than the lithostatic pressure and the ratio of these pressures remains independent of the intrusion width for large laccoliths. Such a result seemed unacceptable for *Kerr and Pollard* [1998], and they generalized their model by including a vertical compressibility for the plate-base interface. However, their numerical results [*Kerr and Pollard*, 1998, Figure 4] show that the magmatic pressure at the center of the intrusion remains non-significantly affected by the width of the intrusion and the base's rigidity. For infinitesimal widths, the model developed here (Figure 2) predicts finite values for the ratio p/q, while the plate approximation of *Kerr and Pollard* [1998, Figure 4], as expected, gave diverging values. These finite ratios are greater than one and probably can also be obtained by constructing asymptotic solutions of the integral equations (13)–(17) in the plane strain case and (24)–(27) in the axisymmetric case.

In the Henry Mountains, the driving pressure ($p - q$) is believed to have ranged up to 700 bars [*Johnson and Pollard*, 1973, Figure 21], while the lithostatic pressure is a linear function of the overburden thickness and is ~1000 bars for a 4-km-thick overburden [*Johnson and Pollard*, 1973, Figure 20]. Thus the potential ratio (p/q) is no more than 1.7 if the thickness is ~4 km. Then it appears from Figure 2 that at the elastic stage of bending the magmatic pressures in the Henry Mountains intrusions were nearly uniform.

In Figure 3 the magma pressure averaged over the crack area, noted $\langle P_m \rangle$, is plotted as a function of the geometrical ratio. Using (18), $\langle P_m \rangle$ is related to the pressure p as follows: For the plane strain case

$$\frac{\langle P_m \rangle}{q} = \frac{n}{n+1}\frac{p}{q}, \tag{29a}$$

For the axisymmetric case

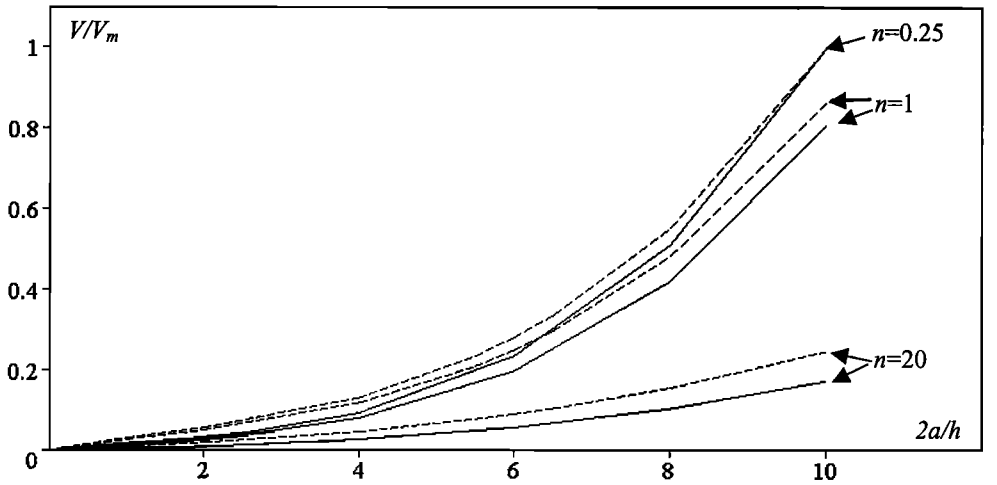

Figure 4. Volume of the intruded magma versus the geometrical ratio. (Solid curves, the plane strain case; dashed curves, the axially symmetric case.)

$$\frac{\langle P_m \rangle}{q} = \frac{n}{n+2}\frac{p}{q}. \tag{29b}$$

In the plane strain case and from (28) and (29) it can be noted that for large intrusions and a varying pressure distribution, the averaged magma pressure is smaller than the lithostatic pressure ($3/4 \leq \langle P_m \rangle/1 \leq 1$ for $0 \leq n < \infty$). Thus, if one makes a vertical cut around the perimeter of the laccolith, the force resulting from the shear stresses exerted on this boundary by the surroundings is upward. Such situations are well known in the beam theory and especially the case of a beam uplifted by a point force.

For small geometrical ratios the averaged magma pressure is greater than the lithostatic pressure and still finite even for infinitesimal width. The crossing point of the various n curves in Figures 3a and 3b corresponds approximately to the ratio $\langle P_m \rangle/q = 1.1$ and is nearly independent of the pressure distribution. In the plane strain case (Figure 3a) and the axially symmetric case (Figure 3b) the crossing point appears when the ratio of the intrusive diameter to the overburden thickness is ~2 and 3, respectively. In the study of the intrusion thickness, presented in section 4.2, this crossing point will be correlated to the transition between a sill and a laccolith.

The curves of the intruded magma volume V, normalized by V_m ($= V(2a/h = 10, n = 0.25)$), versus the geometrical ratio are shown in Figure 4, which is obtained in the case of no material contrast ($\theta = 0$). These curves show that the intruded volume increases quickly when the geometrical ratio increases. Such results can explain the decrease of the magmatic pressure (Figure 3) when the geometrical ratio increases.

4.2. Shapes and Thicknesses

The asymmetry in the vertical displacements above and below the intrusion due to both the free surface and the material contrast is analyzed in Figure 5. In Figure 5 the results correspond to the plane strain case and are qualitatively similar to those of the axially symmetric case. Figure 5a corresponds to a small geometrical ratio ($2a/h = 0.02$) and identical materials above and below the intrusion ($\theta = 0$). Obviously the shapes are essentially symmetric. In Figure 5b, in which $2a/h = 0.02$ and $\theta = +0.33$, the asymmetry is due to the material contrast (i.e., the base is 2 times more rigid than the overburden), and the downward displacements are not negligible. For an intermediate ratio ($2a/h = 2$) and no material contrast, the obtained asymmetry (Figure 5c) is due to the free surface and the depressing of the floor is less important than the roof doming, which begins to be favoured. For a large ratio ($2a/h = 10$) and no material contrast, the shape is essentially laccolithic (Figure 5d) since the displacements below the intrusion are nonsignificant. Shapes similar to those of Figure 5d are also obtained in the case of an overburden two times more rigid than the base ($\theta = -0.33$). When the overburden is 100 times more rigid than the base ($\theta = -0.99$), the roof doming still more important than the floor sinking. Thus the effect of the free surface is preponderant on the material contrast when the geometrical ratio is sufficiently large. As shown in Figure 5e, in which the Dundurs constant is fixed to -0.33 and the geometrical ratio is 0.02, the effect of the material contrast is geologically significant for small geometrical ratios. In that case, the floor depressing is favored to the roof doming, and at smaller geometrical ratios or smaller values of θ the intrusion will be essentially lopolithic. Such result conforms to the field observations [*Corry*, 1988] in that lopoliths form at greater depths than laccoliths. Otherwise and since among the geometrical parameters only the ratio a/h controls the intrusion shapes, Gilbert's concept that lesser overburden should correspond to a smaller radius for laccoliths is confirmed here.

The results shown in Figure 5 can also be used to analyze the effect of the driving pressure distribution on the intrusion shapes. For a crack in an infinite medium and a uniform pressure the analytical result for the vertical displacement U_z, normalized by $U_{z\max}$, the displacement at the center of the crack, is such as $U_z/U_{z\max} = \sqrt{1 - (x/a)^2}$ [*Sneddon*, 1951]. As shown in Figure 5a, the shape obtained with a nearly uniform pressure distribution conforms to the analytical shape except at the peripheries. For large geometrical ratios and uniform pressure the plate-bending model leads to vertical displacements such as $U_z/U_{z\max} = [1 - (x/a)^2]^2$ [*Timoshenko and Woinowsky-Kriegler*, 1959]. As shown in Figure 5d, the shape obtained with the nearly uniform pressure distribution approaches the classical result of a bending plate and is consistent with shapes over major laccolithic intrusions observed in the field. Indeed, over a major laccolith the flexed strata are

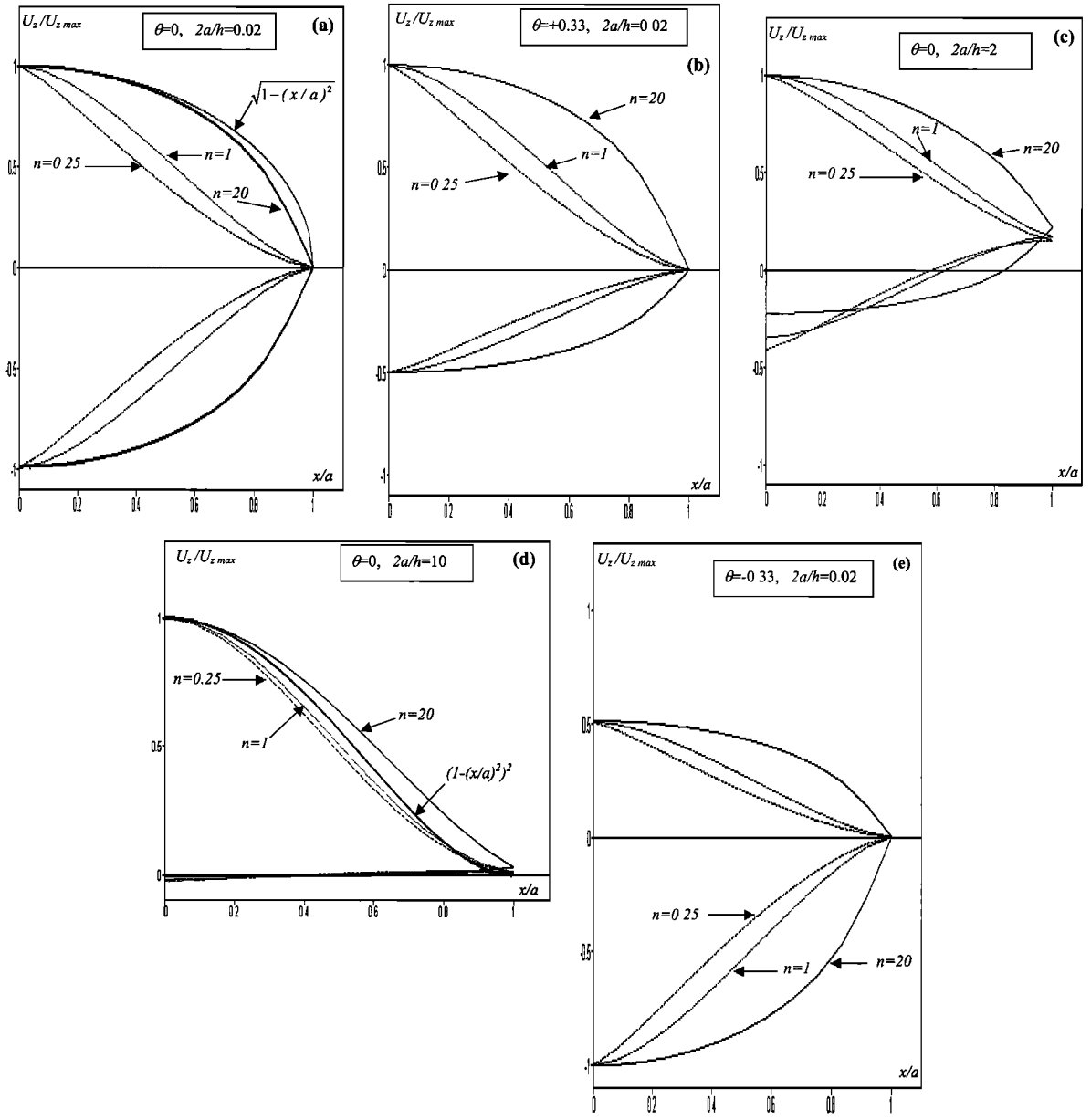

Figure 5. Shapes of the vertical displacements over and below the magmatic intrusion for various geometrical ratios ($2a/h$), material contrasts and pressure distributions. (a) The case of a small geometrical ratio and no material contrast ($\theta = 0$). (b) The case of a small geometrical ratio and an overburden less rigid than the base ($\theta = +0.33$). (c) The case of an intermediate geometrical ratio ($2a/h = 2$) and no material contrast ($\theta = 0$). (d) The case of a large geometrical ratio ($2a/h = 10$) and no material contrast ($\theta = 0$). (e) The case of a small geometrical ratio ($2a/h = 0.02$) and an overburden more rigid than the base ($\theta = -0.33$).

known to have a doubly hinged shape. A central limb of nearly constant dip joins the concave downward upper hinge and the concave upward lower hinge [*Pollard and Johnson*, 1973; *Jackson and Pollard*, 1988, Figure 10; *Jackson and Pollard*, 1990, Figure 2–4]. In Figures 5a–5c, which correspond to small or intermediate geometrical ratios, and on the curves corresponding the nearly uniform pressure, the central limb and the lower hinge are too short and the central limb steeps to almost vertical. Such shapes correspond to earlier stages in the growth of domes like those described by *Jackson and Pollard* [1988, Figures 19a–19c.] With the linear pressure distribution and for any geometrical ratios the current results lead to doubly hinged shapes with a large central limb.

The ratio of the intrusion width ($2a$) to its thickness at the center ($(U_z^1 - U_z^2)(z = 0)$) is plotted in Figure 6 as a function of the geometrical ratio ($2a/h$). The curves in Figure 6, which is obtained in the case of no material contrast ($\theta = 0$), show that an important increase in the thickness of the intrusion relatively to its width begins when the geometrical ratio passes the value 2 in the plane strain case and 3 in the axially symmetric case. These values correspond to the cross points that appeared in Figure 3. The increase in the intrusion thickness detects the transition from sill shape to laccolith shape. This result improves previous analyses concerning the sill-laccolith transition. Indeed, according to *Pollard and Johnson* [1973, p. 348] the transition between a sill and a laccolith

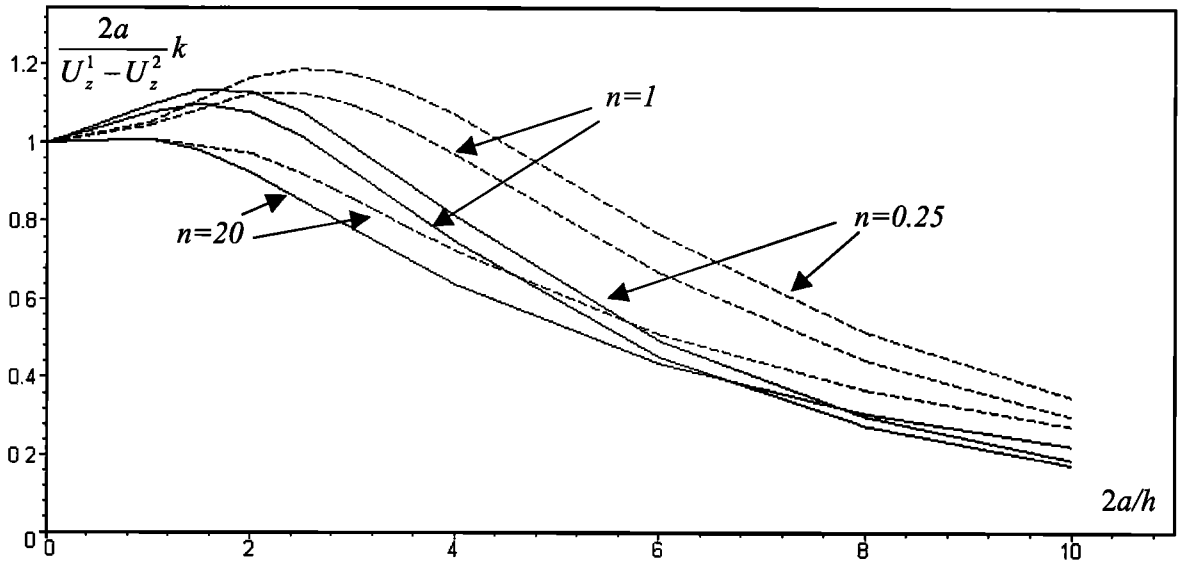

Figure 6. The ratio of the intrusion's width to its thickness at the center versus the geometrical ratio for various values of n ($k = (U_z^1 - U_z^2)/2a$ for $2a/h = 0.02$). (Solid curves, the plane strain case; dashed curves, the axially symmetric case.)

occurs when the ratio of the intrusive diameter to the overburden thickness is ~3.2 in the plane strain case and 3.8 in the axisymmetric case. They obtained these values by equating the displacement of a crack in an infinite medium and the deflection of a thin plate (both of them under uniform magmatic pressure). This way of calculating the geometrical ratios corresponding to the transition between sills and laccoliths is a priori not justified and was criticized by *Pollard and Holzhausen* [1979], who proposed the value of 1.6 for the transition ratio in the plane strain case.

4.3. Application to the Black Mesa Intrusion

The purpose of this application is to demonstrate some of the predictions that can be made with the models presented in this paper. In its present form the Black Mesa intrusion has a circular plane shape with a radius $a = 850$ m. This intrusion is here analyzed using the following data, which are taken from *Pollard and Johnson* [1973, pp. 349–351]: the lithostatic pressure is $q = 650$ bars, the magmatic pressure at the center of the intrusion is $p = 700$ bars, the elastic coefficients of the overburden are such that $B = 2\mu_1/(1 - \nu_1) = 5000$ bars, the total overburden thickness is $h_T = 2700$ m, the thickness attained both above and below the center of the intrusion at the end of the bending stage is $U_z^1 - U_z^2 = 50$ m, and the sill-laccolith transition occurred at an intrusion radius of about $a_{\text{transition}} = 500$ m. The values of a and h_T are estimated by direct measurement, while the other parameters are from field work and some specific analysis. The estimation of the transition radius, $a_{\text{transition}}$, is made on the basis of observations of other sills in the Henry Mountains. The intrusion thickness at the end of the bending stage is defined as the thickness at which the layers over the intrusion would fail by excessive longitudinal strain. In the following and using our models, we look for an estimation of the transition radius and compare this estimation to the available value.

The overburden and base are here considered of the same material, and we suppose that at the end of the bending stage the elasticity solutions remain appropriate. We also suppose that the overburden behaves as a single layer of an unknown effective thickness h, which should be smaller than h_T. For given elastic properties and a lithostatic pressure the models developed in this paper allow the determination of the ratio $(U_z^1 - U_z^2)/a$ for many geometrical ratios $2a/h$ and many driving pressure distributions. Figure 7a shows that only nearly uniform pressures (large n) may reach the ratio $(U_z^1 - U_z^2)/a$ corresponding to the Black Mesa intrusion, and this conforms to our previous conclusion concerning the magmatic pressures in the Henry Mountains intrusions. However, estimates of the magma pressure are generally uncertain. That is, raising of the estimated pressure would allow for lower values of n. To fix the effective thickness, the available ratio p/q should be used. Figure 7b shows that the effective thickness that satisfies the parameters of the Black Mesa intrusion corresponds to the ratio $2a/h = 3.5$. Thus the overburden effective thickness is ~485 m and the sill-laccolith transition occurred at an intrusion radius of about 730 m ($a_{\text{transition}} = 3h/2$ in the axisymmetric model) if the shape of the intrusion was always circular during the emplacement process. However, according to *Pollard and Johnson* [1973, pp. 351–352] the plane shape of the intrusion was not circular early in its development but was roughly elliptical with a long axis parallel to the trend of the feeder. The circular shape was reached after the sill-laccolith transition. When considering that the sill-laccolith transition occurred in a plane strain configuration, the transition radius is 485 m ($a_{\text{transition}} = h$ in the plane strain model), which is not far from the available value.

5. Conclusion

In this study, semianalytical solutions of elasticity problems relevant to the emplacement of magmatic intrusions are constructed including both the elongated intrusion case and the circular one. The difference in elastic constants between the overburden and base is taken into account and is characterized by one of the Dundurs parameters (θ) which is a combination of Poisson's ratios and shear moduli of the two materials. The

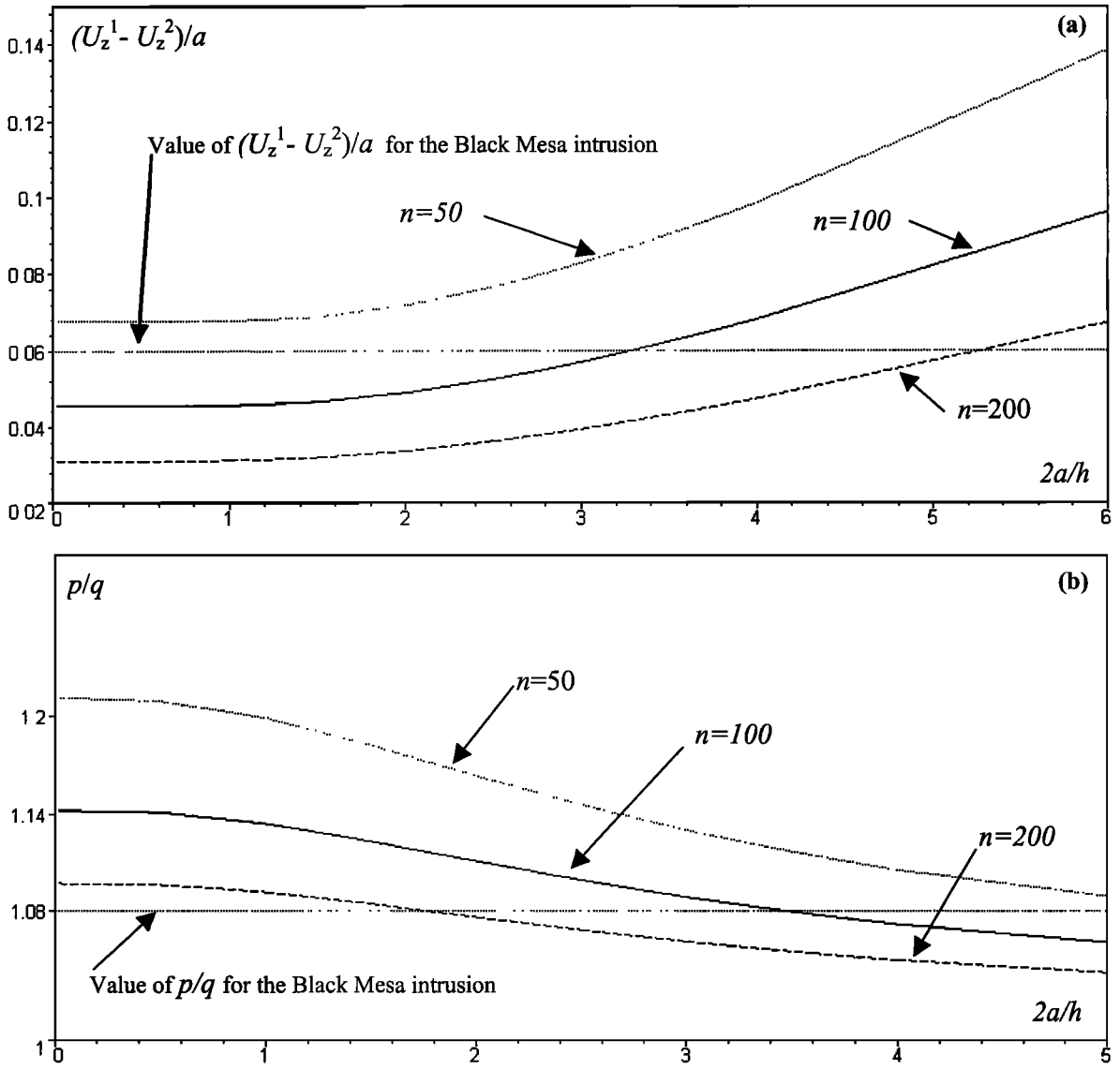

Figure 7. Application to the Black Mesa intrusion. (a) The ratio of the intrusion's thickness to its radius versus the geometrical ratio ($2a/h$) for different nearly uniform pressure distributions. (b) The ratio of the magmatic pressure at the center of the intrusion to the lithostatic pressure versus the geometrical ratio for different nearly uniform pressure distributions.

ratio ($2a/h$) of the intrusion's width to the overburden thickness is also an important parameter in this study. For large ratios and any geologically significant material contrast, the effect of the free surface is such as the shape of the intrusion is essentially laccolithic. The obtained results are also consistent with Gilbert's concept that a lesser overburden should correspond to a smaller laccolith width. The study of intermediate geometrical ratios allowed here the exploration of the sill-laccolith transition. This transition occurs when the roof lifting is favored over the horizontal sill growth. In the plane strain case and the axially symmetric case the transition is found to occur at geometrical ratios, ~2 and 3, respectively. This transition appeared to be independent of the form of the magmatic pressure distribution which is between the nearly uniform case and the nearly point load case. In the Henry Mountains, only nearly uniform pressure distributions are significant. For a given geometrical ratio ($2a/h$), licit ratios of the magma pressure averaged over the intrusion area to the lithostatic pressure are given. These ratios are greater than one for small geometrical ratios and smaller than one for large ratios. For small geometrical ratios a geological realistic material contrast can introduce an asymmetry in the vertical displacements above and below the intrusion. It is shown that for small ratios ($2a/h < 0.02$) and a substrate shear modulus which is 2 times that of the overburden ($\theta = -0.33$), the depressing of the intrusion's floor is more important than the doming of its roof, and thus lopolithic shapes are favored.

Appendix A

A1. Plane Strain Problem

$$B^1(t) = A^1(t)M(t)t(1 - e^{2th} - 2the^{2th}), \quad \text{(A1)}$$

$$C^1(t) = -A^1(t)M(t)e^{2th}(1 - 2th + 2t^2h^2 - e^{2th}), \quad \text{(A2)}$$

$$D^1(t) = A^1(t)M(t)te^{2th}(1 - 2th - e^{2th}), \quad \text{(A3)}$$

$$A^2(t) = A^1(t)M(t)[1 - 2e^{2th}(1 + 2t^2h^2) + e^{4th}], \quad \text{(A4)}$$

$$B^2(t) = tA^2(t), \quad \text{(A5)}$$

$$M(t) = [1 - (1 + 2th + 2t^2h^2)e^{2th}]^{-1}, \quad \text{(A6)}$$

$$E(t) = \frac{4}{\pi}\frac{(1 - \nu_1)}{(1 + \theta)\mu_1}A^1(t)M(t)t\{[1 - 2th + 2t^2h^2 - \theta(1 + 2th + 2t^2h^2)]e^{2th} - e^{4th} + \theta\}. \quad \text{(A7)}$$

A1.1. Proof of equations (13)–(15). Using (A1)–(A6), the boundary condition (7) yields

$$\frac{(1 + \theta)\mu_1}{2(1 - \nu_1)}\int_0 sH(s)\int_0^\infty W(t)J_0(st)\cos(tx)\,dt\,ds = P(x) \quad \text{(A8)}$$

$$W(t) = -\frac{t(1 - 2(1 + 2t^2h^2)e^{2th} + e^{4th})}{[1 - 2th + 2t^2h^2 - \theta(1 + 2th + 2t^2h^2)]e^{2th} - e^{4th} + \theta} \quad \text{(A9)}$$

Equation (A8) is then written as

$$\int_0^a sH(s)\int_0^\infty tJ_0(st)\cos(tx)\,dt\,ds + \int_0^a sH(s)\int_0^\infty [W(t) - t]J_0(st)\cos(tx)\,dt\,ds = \frac{2(1 - \nu_1)}{(1 + \theta)\mu_1}P(x). \quad \text{(A10)}$$

After suitable integration by part in the first integral in (A10), the obtained equation is viewed as an Abel's integral equation and solved for $H(s)$. This results in (13)–(15).

A1.2. Proof of equation (16). Using (11), the contact pressure is expressed as

$$\sigma_{zz}^1(x, 0) = -\int_0^\infty\int_0^a sH(s)W(t)\cos(tx)J_0(ts)\,ds\,dt \quad \text{(A11)}$$

and after integration by parts becomes

$$\sigma_{zz}^1(x, 0) = -aH(a)\int_0^\infty \frac{W(t)}{t}\cos(tx)J_1(ta)\,dt + \int_0^\infty \frac{W(t)}{t}\cos sH'(s)J_1(ts)\,ds\,dt. \quad \text{(A12)}$$

Since $W(t)/t$ tends to 1 when t tends to infinity it is seen that if the contact pressure is not to be singular at $x = a$, then $H(a) = 0$.

A2. Axisymmetric Problem

$$B^1(t) = A^1(t)M(t)t(1 - e^{2th} - 2the^{2th}), \quad \text{(A13)}$$

$$C^1(t) = 2A^1(t)M(t)e^{2th}(\nu_1 - 2\nu_1th + t^2h^2 - \nu_1e^{2th}), \quad \text{(A14)}$$

$$D^1(t) = -A^1(t)M(t)te^{2th}(1 - 2th - e^{2th}), \quad \text{(A15)}$$

$$A^2(t) = A^1(t)N(t)\nu_2(1 - 2\nu_2)[1 - 2e^{2th}(1 + 2t^2h^2) + e^{4th}], \quad \text{(A16)}$$

$$B^2(t) = \frac{1}{2\nu_2}tA^2(t), \quad \text{(A17)}$$

$$M(t) = 2[\nu_1 - (\nu_1 + 2\nu_1th + t^2h^2)e^{2th}]^{-1}, \quad \text{(A18)}$$

$$N(t) = \frac{1}{1 - 2\nu_1}[\nu_1 - (\nu_1 + 2\nu_1th + t^2h^2)e^{2th}]^{-1}, \quad \text{(A19)}$$

$$E(t) = -2\frac{(1 - \nu_1)}{(1 + \theta)\mu_1}A^1(t)N(t)t^3\{[1 - 2th + 2t^2h^2 - \theta(1 + 2th + 2t^2h^2)]e^{2th} - e^{4th} + \theta\}. \quad \text{(A20)}$$

A2.1. Proof of equations (24)–(26). Using (A13)–(A19) and (22), the boundary condition (7) yields

$$\frac{(1 + \theta)\mu_1}{2(1 - \nu_1)}\int_0^a H(s)\int_0^\infty W(t)J_0(xt)\sin(st)\,dt\,ds = P(x) \quad \text{(A21)}$$

$$W(t) = -\frac{t(1 - 2(1 + 2t^2h^2)e^{2th} + e^{4th})}{(1 - 2th + 2t^2h^2 - \theta(1 + 2th + 2t^2h^2))e^{2th} - e^{4th} + \theta}. \quad \text{(A22)}$$

Equation (A21) is then written as

$$\int_0^a H(s)\int_0^\infty tJ_0(st)\sin(sx)\,dt\,ds + \int_0^a H(s)\cdot\int_0^\infty [W(t) - t]J_0(xt)\sin(st)\,dt\,ds = \frac{2(1 - \nu_1)}{(1 + \theta)\mu_1}P(x). \quad \text{(A23)}$$

After suitable integration by parts in the first integral in (A23), the obtained equation is viewed as an Abel's integral equation and solved for $H(s)$, which results in (24)–(26).

A2.2. Proof of equation (27). The contact pressure is expressed as

$$\sigma_{zz}^1(x, 0) = -\int_0^\infty\int_0^a H(s)W(t)\sin(ts)J_0(tx)\,ds\,dt \quad \text{(A24)}$$

and after integration by parts becomes

$$\sigma_{zz}^1(x, 0) = H(a)\int_0^\infty \frac{W(t)}{t}\cos(at)J_0(tx)\,dt - \int_0^\infty \frac{W(t)}{t}J_0(tx)\int_0^a H'(s)\cos(ts)\,ds\,dt. \quad \text{(A25)}$$

From (A25), it is seen that if the contact pressure is not to be singular at $x = a$, then $H(a) = 0$.

Acknowledgments. Comments on drafts of the manuscript by M. J. Rodgers and journal reviewers are gratefully acknowledged.

References

Abé, H., T. Mura, and L. M. Keer, Growth rate of a penny-shaped crack in hydraulic fracturing of rocks, *J. Geophys. Res.*, *81*, 5335–5340, 1976.

Corry, C. E., Laccolith: Mechanics of emplacement and growth, *Spec. Pap., Geol. Soc. Am.*, *220*, 1988.

Dundurs, J., and M. Stippes, Role of elastic constants in certain contact problems, *J. Appl. Mech.*, *37*, 965–970, 1970.

Erdogan, F., Bonded dissimilar materials containing cracks parallel to the interface, *Eng. Fract. Mech.*, *3*, 231–240, 1971.

Gilbert, G. K., Report on the Geology of the Henry Mountains, U.S. Geogr. and Geol. Surv. of Rocky Mt. Reg., Washington, D.C., 1877.

Guterman, V. G., Y. A. Fialko, and Y. M. Khazan, Dome structures over sill-like crustal structures: A numerical model of preseismic uplift, 1, *Geophys. J.*, Engl. Transl., *16*(4), 209–226, 1996.

Jackson, M. D., and D. D. Pollard, The Laccolith-Stock controversy: New results from the southern Henry Mountains, Utah, *Geol. Soc. Am. Bull.*, *100*, 117–139, 1988.

Jackson, M. D., and D. D. Pollard, Flexure and faulting of sedimentary host rocks growth of igneous domes, Henry Mountains, Utah, *J. Struct. Geol.*, *12*, 185–206, 1990.

Johnson, A. M., and D. D. Pollard, Mechanics of growth of some laccolithic intrusions in the Henry Mountains, Utah, I, Field observations, Gilbert's model, physical properties and flow of magma, *Tectonophysics*, *18*, 261–309, 1973.

Keer, L. M., and K. Chantaramungkorn, Loss of contact between a layer and a half-space, *J. Elast.*, *2*, 191–197, 1972.

Keer, L. M., J. Dundurs, and K. C. Tsai, Problems involving a receding contact between a layer and a half space, *J. Appl. Mech.*, *39*, 1115–1120, 1972.

Kerr, A. D., and D. D. Pollard, Toward more realistic formulations for the analysis of laccoliths, *J. Struct. Geol.*, *2*, 1783–1793, 1998.

Pollard, D. D., and G. Holzhausen, On the mechanical interaction between a fluid-filled fracture and the Earth's surface, *Tectonophysics*, *53*, 27–57, 1979.

Pollard, D. D., and A. M. Johnson, Mechanics of growth of some laccolithic intrusions in the Henry Mountains, Utah, II, Bending and failure of overburden layers and sill formation, *Tectonophysics*, *18*, 311–354, 1973.

Sneddon, I. N., *Fourier Transforms*, McGraw-Hill, New York, 1951.

Srivastava, K. N., and K. Singh, The effect of penny-shaped crack on the distribution of stress in a semi-infinite solid, *Int. J. Eng. Sci.*, *7*, 469–490, 1969.

Timoshenko, S., and S. Woinowsky-Krieger, *Theory of Plate and Shells*, McGraw-Hill, New York, 1959.

Turcotte, D. L., and G. Shubert, *Geodynamics: Application of Continuum Physics to Geological Problems*, John Wiley, New York, 1982.

L. M. Keer, Department of Civil Engineering, Northwestern University, Evanston, IL 60208. (l-keer@northwestern.edu)

H. Zenzri, Departement de Genie Civil, Ecole Nationale d'Ingenieurs de Tunis, B.P. 37, 1002 Tunis, Tunisia. (hatem.zenzri@enit.rnu.tn)

(Received June 5, 2000; revised March 8, 2001;
accepted March 21, 2001.)